

# Quantum transport in a curved one-dimensional quantum wire with spin-orbit interactions

Erhu Zhang, Shengli Zhang, Qi Wang<sup>1</sup>

<sup>1</sup>*Department of Applied Physics, Xi'an Jiaotong University,  
Xi'an 710049, P. R. China*

(Dated: October 10, 2018)

The one-dimensional effective Hamiltonian for a planar curvilinear quantum wire with arbitrary shape is proposed in the presence of the Rashba spin-orbit interaction. Single electron propagation through a device of two straight lines conjugated with an arc has been investigated and the analytic expressions of the reflection and transmission probabilities have been derived. The effects of the device geometry and the spin-orbit coupling strength  $\alpha$  on the reflection and transmission probabilities and the conductance are investigated in the case of spin polarized electron incidence. We find that no spin-flip exists in the reflection of the first junction. The reflection probabilities are mainly influenced by the arc angle and the radius, while the transmission probabilities are affected by both spin-orbit coupling and the device geometry. The probabilities and the conductance take the general behavior of oscillation versus the device geometry parameters and  $\alpha$ . Especially the electron transportation varies periodically versus the arc angle  $\theta_w$ . We also investigate the relationship between the conductance and the electron energy, and find that electron resonant transmission occurs for certain energy. Finally, the electron transmission for the incoming electron with arbitrary state is considered. For the outgoing electron, the polarization ratio is obtained and the effects of the incoming electron state are discussed. We find that the outgoing electron state can be spin polarization and reveal the polarized conditions.

PACS numbers: 72.25.-b, 73.21.Hb, 71.70.Ej

## I. INTRODUCTION

Recently, a new subdiscipline of condensed matter physics, spintronics, is emerging rapidly and generating great interests<sup>[1,2]</sup>. Much attention has been focused, especially, on the spin-dependent transport dominated by the spin-orbit interaction (SOI)<sup>[3,4]</sup> in the low dimensional semiconductor nanostructures, such as wires, rings, spirals, and other structures. For example, the influence of spin on electrons moving in a mesoscopic ring have been studied in several contexts<sup>[5–10]</sup> since the original proposal of the spin field effect transistor by Datta and Das<sup>[11]</sup>.

On the other hand, many low-dimensional systems are curvilinear and more complicated in geometry, such as the V-shaped quantum wire<sup>[12]</sup>, the spiral inductors<sup>[13]</sup>, nanotubes<sup>[14]</sup>, and so on. Due to the potential of providing new physical features and new functionalities for electronic devices<sup>[15]</sup>, the effects of the curvilinear geometry on electronic states and electron transports are the subjects of many recent works<sup>[16–20]</sup>. Especially, the influence of geometry on the SOI is considered by some groups<sup>[21,22]</sup>. The systems concerned are quasi-one-dimensional circles or two-dimensional (2D) nanostructures. However, for one dimensional (1D) system, the electron behavior in curved quantum wires with arbitrary shape is still a challenging question. The purpose of this paper is to study the curvature effects on the electron transport through a 1D curved nanostructure taking into account the SOI.

This paper is organized as follows. In Sec. II, we investigate a 1D planar curvilinear quantum wire with arbitrary shape. The effective Hamiltonian is derived using perturbation theory. In Sec. III we study the one-electron energy spectrum and eigenstates of curvilinear quantum wire. Then we consider the corresponding transmission of electrons. A detailed numerical discussion is given. Conclusions and remarks follow in Sec. IV.

## II. EFFECTIVE HAMILTONIAN FOR A 1D PLANAR CURVILINEAR QUANTUM WIRE

We consider the adiabatic motion of electrons bounded on a planar quantum wire as shown in Fig. 1(a). Under the effective-mass approximation, the Schrödinger equation for an electron in the presence of Rashba SOI<sup>[3]</sup> is given by

$$\left[ \frac{\mathbf{p}^2}{2m} + V(\mathbf{r}) + \hat{H}_{SO} \right] \Psi = E\Psi, \quad (1)$$
$$\hat{H}_{SO} = \alpha \hat{\sigma} \cdot \mathbf{n} \times \mathbf{p},$$

where  $m$  is the effective electron mass,  $\hat{\sigma}$  is the Pauli matrices and  $\mathbf{n}$  is the surface normal. Here  $V(\mathbf{r})$  represents the potential which confines electrons to the wire, while the Rashba term results from the asymmetric confinement along

the direction perpendicular to the plane. The parameter  $\alpha$  is the Rashba parameter which represents the average electric field along the  $\mathbf{n}$  direction.

In order to obtain the effective Hamiltonian for electrons on a 1D wire, we take the same approach as da Costa's<sup>[23]</sup>. Let  $\mathbf{a}(s)$  parametrically specify the 1D planar curve where  $s$  is the arc length along the curve. Any point in the surface surrounding the curve can be expressed as follows:

$$\mathbf{r}(s, u) = \mathbf{a}(s) + u\mathbf{b}(s), \quad |u| \leq \frac{\varepsilon}{2}, \quad (2)$$

where  $\mathbf{b}(s) = \frac{1}{\kappa} \frac{d^2\mathbf{a}(s)}{ds^2}$  is the normal of  $\mathbf{a}(s)$  and  $\kappa = |d^2\mathbf{a}(s)/ds^2|$  is the curvature of the curve, the curve width  $\varepsilon$  is small and is assumed to be less than the curvature radii. The twosome  $\{s, u\}$  forms a curvilinear coordinate system in the 2D plane. The concerned electron moving along the wire is confined near the curve  $\mathbf{a}(s)$  in the normal direction by a potential  $V(u)$ .

In this curvilinear coordinate system, the corresponding metric tensor is

$$G_{ij} = \begin{pmatrix} (1 - u\kappa)^2 & 0 \\ 0 & 1 \end{pmatrix}. \quad (3)$$

So the wave function should be normalized according to the condition

$$\int |\Psi|^2 \sqrt{G} ds du = 1, \quad G = \det[G_{ij}]. \quad (4)$$

It is convenient to introduce a new function  $\Psi' = \Psi G^{1/4}$  to eliminate  $\sqrt{G}$  from the area element in the normalization condition.

After some substitution, the Schrödinger equation is rewritten and the new function  $\Psi'$  is separable in  $s$  and  $u$ ,  $\Psi'(s, u) = \Phi(s)R(u)$ , since  $V(u)$  does not depend on  $s$ . The eigenfunction  $R(u)$  depicts the transversal motion in the confining potential  $V(u)$ . For small  $\varepsilon$  or deep confining potential, the confining energy in the transversal direction is much larger than the SO energy and the kinetic energy in the longitudinal direction. This allows us to divide the electron transversal motion from the longitudinal motion and the SOI. In the limit of 1D wires,  $\varepsilon \rightarrow 0$ , the electron will be in the lowest transversal mode  $R_0(u)$ . Then we have an infinitely degenerate set of states  $\Psi'_n(s, u) = \Phi_n(s)R_0(u)$  where the  $\Phi_n(s)$  denote a complete set of spinors in the  $s$  direction. Accordingly the corresponding effective Hamiltonian can be found in a way similar to Ref. 24.

In order to obtain the exact expression of the effective Hamiltonian, we have to calculate the lowest transversal mode for a given confining potential. For generality and simplicity, we assume the confining potentials to be symmetric: for example, the harmonic potential [ $V(u) = \frac{1}{2}Ku^2$ ], the hard-wall potential or the  $\delta(u)$  potential. We find that all these different potentials give the same results as a result of the symmetry of the potential. The 1D effective Hamiltonian in the presence of SOI for a planar quantum wire is given by

$$\hat{H}_{1D} = -\frac{\hbar^2}{2m} \frac{\partial^2}{\partial s^2} - \frac{\hbar^2 \kappa^2}{8m} - i\alpha \left[ \sigma_b \frac{\partial}{\partial s} - \frac{1}{2} \sigma_t \kappa \right], \quad (5)$$

where  $\sigma_b = \hat{\sigma} \cdot \mathbf{b}$  and  $\sigma_t = \hat{\sigma} \cdot \mathbf{t} = \hat{\sigma} \cdot \frac{d\mathbf{a}(s)}{ds}$ , expressed by the usual Pauli spin matrices  $\hat{\sigma}_{x,y,z}$ , are the spin matrices on the normal and tangent direction in the curvilinear coordinate respectively. Here we have redefined  $\alpha$  ( $\alpha \rightarrow \hbar\alpha$ ). Obviously, the equation gives an effective geometric potential term  $V_{eff}(s) = -\hbar^2 \kappa^2 / 8m$  in agreement with the term given by da Costa<sup>[23]</sup>.

Specially the last term in Eq. (5)

$$\hat{H}_{1D,SO} = -i\alpha \left[ \sigma_b \frac{\partial}{\partial s} - \frac{1}{2} \sigma_t \kappa \right], \quad (6)$$

stands for the Rashba SOI in a planar curved quantum wire. It can be easily seen that the geometry of the wire, via the curvature  $\kappa$ , has influence on the SOI. Note that this 1D SOI Hamiltonian is universal for planar wire with arbitrary shape. As a consequence, we can get the corresponding Hamiltonian for a ring which is the same as Meijer *et al*'s<sup>[24]</sup>.

### III. QUANTUM TRANSPORT IN A 1D PLANAR CURVILINEAR QUANTUM WIRE

The structure of the device we consider is shown schematically in Fig. 1(b), consisting of two straight lines conjugated with an arc of a circumference<sup>[25,26]</sup>. Due to the presence of geometric potential, the curved section can be represented as a rectangular potential well (see Fig. 1(d)) with a width  $\theta_w \rho$  and a depth  $-\hbar^2/(8m\rho^2)$ , where  $\rho$  is the radius of the circumference and  $\theta_w$  is the angle between two rectilinear parts of the wire. There exists one and only one bound state for  $\theta_w < \pi$  in such a system<sup>[15]</sup>. In order to study the problem of electron transportation, we need to investigate the eigenstates of this system first.

#### A. Eigenstates and Energy Spectrum

For convenience, the device is divided into three parts as shown in the Fig. 1(c), and the two straight lines are assumed to be semi-infinite. To take into account the geometrical effects, the SOI is considered for all the three sections. Using the above 1D effective Hamiltonian, we can easily write the Hamiltonians for each part. In the selective coordinate of panel (c) in Fig. 1, they read

$$\begin{aligned}\hat{H}_1 &= -\frac{\hbar^2}{2m} \frac{\partial^2}{\partial s^2} - i\alpha\sigma_{b_1} \frac{\partial}{\partial s}, \quad s \in (-\infty, 0), \\ \hat{H}_2 &= -\frac{\hbar^2}{2m\rho^2} \frac{\partial^2}{\partial \theta^2} - \frac{\hbar^2}{8m\rho^2} - \frac{i\alpha}{\rho} [\sigma_{b_2} \frac{\partial}{\partial \theta} - \frac{1}{2}\sigma_{t_2}], \quad \theta \in [0, \theta_w], \\ \hat{H}_3 &= -\frac{\hbar^2}{2m} \frac{\partial^2}{\partial s^2} - i\alpha\sigma_{b_3} \frac{\partial}{\partial s}, \quad s \in (\theta_w\rho, \infty),\end{aligned}\tag{7}$$

where we have introduced the polar angle  $\theta$  for the second part and substituted  $\theta$  for  $s$ . The spin operators are in the forms

$$\begin{aligned}\sigma_{b_1} &= -\sigma_x, \quad \sigma_{b_3} = -\sigma_x \cos \theta_w - \sigma_y \sin \theta_w, \\ \sigma_{b_2} &= -\sigma_x \cos \theta - \sigma_y \sin \theta, \quad \sigma_{t_2} = -\sigma_x \sin \theta + \sigma_y \cos \theta.\end{aligned}\tag{8}$$

We label the eigenstates of the system  $\Phi_{j;\lambda}^{k,\mu}$  where  $j = 1, 2, 3$  denote the corresponding region of the device respectively,  $\lambda = \pm$  indicates the direction of motion along the wire and  $\mu = \pm$  is the spin states.

For the two parts of straight line, the energy spectrum  $E_{1,3}^\mu$  and unnormalized eigenstates  $\Phi_{1;\lambda}^{k,\mu}$  and  $\Phi_{3;\lambda}^{k,\mu}$  are found to be

$$E^\mu = \frac{\hbar^2 k^2}{2m} - \mu\alpha k,\tag{9}$$

$$\Phi_{1;\lambda}^{k,\mu} = e^{i\lambda ks} \chi_1^\zeta, \quad \Phi_{3;\lambda}^{k,\mu} = e^{i\lambda ks} \chi_3^\zeta,\tag{10}$$

where  $\zeta$  takes  $+$  at  $\lambda = \mu$ , or else  $\zeta = -$ . Here the spinors are given by

$$\chi_1^\pm = \begin{pmatrix} \frac{\sqrt{2}}{2} \\ \pm \frac{\sqrt{2}}{2} \end{pmatrix}, \quad \chi_3^\pm = \begin{pmatrix} \frac{\sqrt{2}}{2} \\ \pm \frac{\sqrt{2}}{2} e^{i\theta_w} \end{pmatrix}.\tag{11}$$

Here we take the wave vector  $k \geq 0$ .

For the second part, i.e. the curved section, the corresponding eigenfunctions and eigenvalues are obtained similarly as

$$\Phi_{2;\lambda}^{n,\mu} = e^{i\lambda n\theta} \chi_2^\zeta,\tag{12}$$

where the orbit quantum number  $n \geq 0$  and  $\zeta$  is the same as Eq. (10). Here the spinors  $\chi_2^\zeta$  take the forms of

$$\chi_2^+ = \begin{pmatrix} \sin \frac{\varphi}{2} \\ e^{i\theta} \cos \frac{\varphi}{2} \end{pmatrix}, \quad \chi_2^- = \begin{pmatrix} \cos \frac{\varphi}{2} \\ -e^{i\theta} \sin \frac{\varphi}{2} \end{pmatrix},\tag{13}$$

where the angle  $\varphi$ , satisfying  $\varphi \rightarrow \pi/2$  in the adiabatic limit  $\rho \rightarrow \infty$ , is given by  $\tan \varphi = -\omega/\Omega$  with  $\Omega = \hbar^2/(2m\rho^2)$  and  $\omega = \alpha/\rho$ . The associated eigenenergies read

$$E_{2;\lambda}^\mu = \Omega[(n + \lambda\frac{1}{2})^2 - \mu(n + \lambda\frac{1}{2})\sqrt{1 + \frac{\omega^2}{\Omega^2}}]. \quad (14)$$

We will use these results in the following section to study the transport properties.

## B. Transmission & Reflection Coefficients and Conductance

We consider an electron which is transported from the 1st section to the 3rd section through the arc to study the transport properties of the system. In this case it is appropriate to apply a spin-dependent version of the Griffith's boundary conditions<sup>[27,28]</sup> at the intersections. This reduces the electron transport through the device to an exactly solvable 1D scattering problem. Accordingly there are two boundary conditions: (i) the wave functions must be continuous, and (ii) the spin probability current density must be conserved.

Due to the conservation of energy, the total wave functions corresponding to the same energy in the three regions can be written as linear combination of the corresponding eigenstates. In the presence of Rashba coupling, the energy splitting is such that electrons with Fermi energy  $E_F$  have different wave numbers depending on spin ( $\mu$ ) and the direction of motion ( $\lambda$ ). The quantities  $k$  and  $n$  are obtained by solving  $E_\lambda^\mu = E_F$  in Eq. (9) and Eq. (14) respectively. Let the incoming electron wave function  $\Phi_{in}$  be  $\cos(\phi)\Phi_{1;+}^{k,+} + \sin(\phi)\Phi_{1;+}^{k',-}$ , where the parameter  $\phi$  determines the probability amplitude of each eigenstate, the wave functions of the device read

$$\begin{aligned} \Phi_1 &= \cos(\phi)\Phi_{1;+}^{k,+} + \sin(\phi)\Phi_{1;+}^{k',-} + r_+\Phi_{1;-}^{k',-} + r_-\Phi_{1;-}^{k,+}, \\ \Phi_2 &= c_1\Phi_{2;+}^{n1,+} + c_2\Phi_{2;-}^{n2,+} + d_1\Phi_{2;+}^{n3,-} + d_2\Phi_{2;-}^{n4,-}, \\ \Phi_3 &= t_+\Phi_{3;+}^{k,+} + t_-\Phi_{3;+}^{k',-}, \end{aligned}$$

respectively. Here  $r_\pm$  stands for the reflection coefficients while  $t_\pm$  are transmission coefficients for spin polarization  $\chi^\pm$  respectively, and  $c_1, c_2, d_1, d_2$  are the corresponding coefficients of the wave function.

Using the boundary conditions, we can determine the reflection and transmission probabilities which are expressed as the following forms:

$$R_+ = |r_+|^2 = \frac{4[(A^2 - B^2) \sin(\beta\theta_w) \cos \phi]^2}{(A+B)^4 + (A-B)^4 - 2(A^2 - B^2)^2 \cos(2\beta\theta_w)}, \quad (15)$$

$$R_- = |r_-|^2 = \frac{4[(A^2 - B^2) \sin(\beta\theta_w) \sin \phi]^2}{(A+B)^4 + (A-B)^4 - 2(A^2 - B^2)^2 \cos(2\beta\theta_w)}, \quad (16)$$

$$T_+ = |t_+|^2 = \frac{8A^2B^2(\cos^2 \phi + \cos \varphi \cos(\varphi - 2\phi) \cos[(1 + 2\gamma)\theta_w] + \sin^2(\varphi - \phi))}{(A+B)^4 + (A-B)^4 - 2(A^2 - B^2)^2 \cos(2\beta\theta_w)}, \quad (17)$$

$$T_- = |t_-|^2 = \frac{8A^2B^2(\cos^2(\varphi - \phi) - \cos \varphi \cos(\varphi - 2\phi) \cos[(1 + 2\gamma)\theta_w] + \sin^2 \phi)}{(A+B)^4 + (A-B)^4 - 2(A^2 - B^2)^2 \cos(2\beta\theta_w)}, \quad (18)$$

satisfying the normalization condition,  $R_+ + R_- + T_+ + T_- = 1$ . Here we have introduced  $A = \sqrt{(\frac{\alpha}{\hbar})^2 + \frac{2E_F}{m}}$ ,  $B = \sqrt{(\frac{\alpha}{\hbar})^2 + \frac{2(E_F+V)}{m}}$  and  $V = \Omega/4$ . The parameter  $\beta$  and  $\gamma$  are defined by  $\beta = \frac{B\hbar}{2\rho\Omega}$  and  $\gamma = -\frac{1}{2} + \frac{1}{2}\sqrt{1 + \frac{\omega^2}{\Omega^2}}$ , respectively.

Finally, the conductance in mesoscopic structures can be expressed by means of the Landauer conductance formula which in our case reads

$$G = G_0 \sum_{\mu=\pm} T_\mu = G_0 \frac{16A^2B^2}{(A+B)^4 + (A-B)^4 - 2(A^2 - B^2)^2 \cos(2\beta\theta_w)}, \quad (19)$$

where the conductance quantum  $G_0 = e^2/h$ .

### C. Numerical Results

For numerical calculation, we consider the curved 1D quantum channels based on InAs. The electrons at the Fermi level in InAs have the effective mass  $m = 0.023m_0$  and the Fermi energy  $E_F = 11.13$  meV. From Eqs. (15-18) and (19), we know that the device geometry, i.e. the radius  $\rho$  of the arc and the angle  $\theta_w$ , will affect the electron transmission. By using specific fabrication method, the scale of  $\rho$  is chosen over a wide range:  $\sim 10 - 1000$  nm. While  $|\theta_w| \leq \pi$  to avoid intersection. In addition, the SO strength  $\alpha$  is assumed to be a tunable quantity too. For example, the SOI strength  $\alpha$  can be controlled by a gate voltage with typical values in the range  $(5 \sim 20) \times 10^{-12}$  eVnm within an InGaAs-based 2D electron gas<sup>[29,30]</sup>.

First of all, we investigate the transmission of single incident electron with the polarized spin. The incoming electron state is chosen to be  $\Phi_{in} = \Phi_{1,+}^{k,+}$ , i.e.  $\phi = 0$ . So one can find that the reflection probability  $R_- = 0$ . This means that there are no spin-flip process when the electron is reflected at the first junction. Another choice of the reversed electron spin incoming states will give the analogous results.

We investigate the relationship of reflection and transmission probabilities on the radius  $\rho$  shown in Fig. 2. Panel (a-c) are for different values of SOI strength  $\alpha$  and fixed  $\theta_w = \pi/2$ , while panel (d-f) are for different  $\theta_w$  at a fixed  $\alpha$ . From these figures, one can see that the electron is reflected completely at  $\rho = 0$ . This is induced by our model that the geometric potential becomes infinite, i.e.  $V_{eff}(s) = -\infty$ , when  $\theta_w \neq 0$  and  $\rho = 0$ . In fact, the quantum wire has the width, so the radius  $\rho$  can not achieve to zero for the condition of a smooth transition. Thereby this result may not be measurable.

We only deal with the conditions of  $\rho \geq 15$  nm. Generally speaking, the reflection probabilities are very small. As  $\rho$  increases, we find that the reflection probabilities  $R_+$  decrease to zero quickly and the transmission probabilities  $T_+ \rightarrow 1$  and  $T_- \rightarrow 0$ . For  $R_+$ , the profiles of curves are slightly affected by the SO coupling and mainly determined by the angle  $\theta_w$  in panels (a) and (d). From Eqs. (15-18), one can see that the SO strength  $\alpha$  shows its effect through the two parameters  $A$  and  $B$ . Considering the ranges of all of the physical quantities, the term consisted  $\alpha$  is found to be smaller than other terms by three orders of magnitude at least. While for  $T_+$  and  $T_-$ , another parameter  $\gamma$  need to be considered. So both the angle  $\theta_w$  and the SOI can affect the profiles of the curves obviously, as seen in panels (b-c) and (e-f).

Figure 3 shows the reflection and transmission probabilities as function of the angle  $\theta_w$  for several  $\rho$  and  $\alpha$ . It is obvious that the profiles of the curves are symmetric on both sides of  $\theta_w = 0$ . For  $\theta_w = 0$ , we get  $R_+ = T_- = 0$  and  $T_+ = 1$  as expected. In our model, the 2nd section of the device vanishes and the device becomes a whole straight line when  $\theta_w = 0$ . Then the Hamiltonians  $\hat{H}_1$  and  $\hat{H}_3$  in Eq. (7) take the same form, the electron state should have no change through the process of transmission.

In Fig. 3, the reflection and transmission probabilities are shown to be periodic functions. From equations (15-18), the periods of the reflection and transmission probabilities are derived as

$$P_{ref} = \frac{\pi}{\beta}, \quad (20)$$

$$P_{tra} = \frac{2\pi}{1 + 2\gamma}. \quad (21)$$

The amplitudes can also be calculated. For example, the amplitude of  $R_+$  is  $(A^2 - B^2)/(A^2 + B^2)$ . Due to the same reason as Fig. 2, the profiles of  $R_+$  vs.  $\theta_w$ , including the periods and the amplitudes, are mainly determined by  $\rho$ .

We plot the dependences of the probabilities on the SOI  $\alpha$  for different  $\theta_w$  and  $\rho$  in Figure 4. Those oscillation vs.  $\alpha$ , influenced by the device geometry, remain for all of the curves. As increasing the SO strength, the SOI is enhanced and can weaken the geometric potential. So one can find that the reflection probabilities  $R_+$  tend to zero and the transmission probabilities  $T_+ \rightarrow 1$  and  $T_- \rightarrow 0$  with the increasing  $\alpha$ . When the SOI is absent, the spin state of the outgoing electron is mainly determined by the angle  $\theta_w$ .

Now we turn to the electron conductance. Figs. 5(a)-(b) show the conductance vs.  $\rho$  for different set of  $\theta_w$  and  $\alpha$ . As increasing  $\rho$ , the conductance increases rapidly and goes to  $G_0$  oscillatorily. The changes are mainly effected by the angle  $\theta_w$ . While the relationships of the conductance to the angle  $\theta_w$ , plotted in Figs. 5(c) and 5(d). Obviously, one can see that the conductance is periodical and symmetrical. Finally the dependences of the conductance on  $\alpha$  are shown in Figs. 5(e) and 5(f). The conductance shows oscillation and goes to  $G_0$  along with the increasing SOI strength. As a whole, we get  $G = G_0(1 - R_+)$  using the normalization condition. So the conductance has the similar behavior with the reflection probability  $R_+$ . For further quantitative analysis, we can see that the effects of the device geometry and the SOI are very small and the conductance shows a periodic variation in the  $10^{-4}$ . So these effects on the conductance may be difficult to be observed.

Furthermore, we consider the electron energy in a wide range, not only localized on the Fermi level. Fig. 6 shows the relationship of the conductance versus the electron energy  $E$  in units of  $E_F$  for different values of the SOI strength

$\alpha$ , the angle  $\theta_w$  and the radius  $\rho$ . One can see that the conductance also has the behavior of oscillation and goes to  $G_0$  with the increase of  $E$ . Especially, there are resonant transmissions at certain energy, similar to the scattering problem of typical square well potential.

Finally, we turn to the incoming electron with the mixed state. From Eq. (19), One can easily see that the conductance is independent of the parameter  $\phi$ . In order to study the influence on the transmission for different incoming electron state, we calculate the polarization ratio  $\tau = (T_+ - T_-)/(T_+ + T_-)$  for the outgoing electron. Considering Eqs. (17) and (18), the polarization ratio  $\tau$  takes the form

$$\tau = \frac{T_+ - T_-}{T_+ + T_-} = \cos(\varphi) \cos(\varphi - 2\phi) \cos[(1 + 2\gamma)\theta_w] + \sin(\varphi) \sin(\varphi - 2\phi). \quad (22)$$

Fig. 7 shows the dependences of  $\tau$  on the parameter  $\phi$  for different values of  $\rho$ ,  $\alpha$  and  $\theta_w$ . It is obvious that the profiles of all curves are periodical on  $\phi$ . The period of the polarization ratio  $\tau$  can be found to be  $\pi$  through Eq. (22). The outgoing electron state can be spin polarized when we choose the appropriate parameters. Especially for the spin polarized incident electron, such as  $\phi = 0$ , we investigate the relationship of the polarization ratio  $\tau$  on the device geometry and the SOI shown in Fig. 8. We find that the spin state of the outgoing electron can also be polarized and just rotated around the  $\mathbf{n}$  direction with the angle  $\theta_w$  as the condition of  $\cos[(1 + 2\gamma)\theta_w] = 1$  is satisfied.

#### IV. CONCLUSIONS AND REMARKS

In conclusion, we have derived the 1D effective Hamiltonian for a planar curvilinear quantum wire in the presence of Rashba SOI. The 1D form of the Rashba SOI is obtained analytically. Then we consider the electron transport in a quantum wire consisting of two straight lines conjugated with an arc of a circumference. For the electron transportation of spin polarized incidence, we calculate the reflection and transmission probabilities and find that the electron transmission is influenced by three parameters: the device geometry ( $\theta_w$  and  $\rho$ ) and the SOI strength  $\alpha$ . The relationships between them are discussed in detail through numerical analysis. The device geometry can influence the electron transportation obviously, so does the SO strength  $\alpha$  except for the electron reflection. There is no spin-flip reflection for the device. The general behavior of oscillating versus  $\rho$ ,  $\theta_w$  or  $\alpha$  are found, especially for the angle  $\theta_w$  the electron transportation shows the periodic character. Using the Landauer formalism, we obtain that the conductance varies near  $G_0$  and goes to  $G_0$  oscillatorily. The relationship of the conductance vs. the electron energy is also investigated. The electron resonant transmissions occur at some certain energy. Finally, we study the influence of the incoming electron state on the electron transmission, especially the spin polarization ratio for the outgoing electron. We can achieve the rotated spin polarized electron output under certain conditions.

There is one point that should be noted here. In our system, the SOI is considered for the whole device for the sake of the geometrical effects. This also makes the SOI controllable through the electron field easily. On the side, the system without the SOI on the two straight lines is also investigated and will be published later. Even so, the study does give us one way to modulate the electron transmission through the correlative parameters, especially the device geometry. As an example, the device is placed on an elastomeric substrate, then the quantum wire can deform in company with the substrate. Thereby the wire geometry changes when the substratum deforms; accordingly the electron transmission changes. We may determine the deformation if we can detect the changes of the electron transmission. Furthermore, this study also suggests that we may construct the custom-built device through the geometry method.

We thank S. Zhao, L. Zhang, R. Liang, Y. Liu, and Z. Yao for helpful discussions. This work is supported by NSF of China under Grant No. 10374075. E. Zhang is also supported by the Doctoral Foundation Grant of Xi'an Jiaotong University (XJTU) No. DFXJTU2004-10 and by the NSF of XJTU (Grant No. 0900-573042).

- 
- <sup>1</sup> S. A. Wolf, D. D. Awschalom, R. A. Buhrman, J. M. Daughton, S. V. Molnar, M. L. Roukes, A. Y. Chtchelkanova, and D. M. Treger, *Science* 294, 1488(2001).
  - <sup>2</sup> L. Žutić, J. Fabian, and S. Das Sarma, *Rev. Mod. Phys.* 76, 323(2004).
  - <sup>3</sup> Yu. A. Bychkov and E. I. Rashba, *Pis'ma Zh. Eksp. Teor. Fiz.* 39, 66(1984) [*JETP Lett.* 39, 78(1984)].
  - <sup>4</sup> Q. F. Sun and X. C. Xie, *Phys. Rev. B* 71, 155321(2005).
  - <sup>5</sup> Taeseung Choi, Sam Young Cho, Chang-Mo Ryu, and Chul Koo Kim, *Phys. Rev. B* 56, 4825(1997).
  - <sup>6</sup> J. Nitta, F. E. Meijer, and H. Takayanagi, *Appl. Phys. Lett.* 75, 695(1999).
  - <sup>7</sup> B. Molnár, F. M. Peeters, and P. Vasilopoulos, *Phys. Rev. B* 69,155335(2004).
  - <sup>8</sup> P. Földi, B. Molnár, M. G. Benedict, and F. M. Peeters, *Phys. Rev. B* 71, 033309(2005).
  - <sup>9</sup> U. Aeberhard, K. Wakabayashi, and M. Sigrist, *Phys. Rev. B* 72, 075328(2005).

- <sup>10</sup> X. F. Wang and P. Vasilopoulos, Phys. Rev. B 72, 165336(2006).
- <sup>11</sup> S. Datta and B. Das, Appl. Phys. Lett. 56, 665(1990).
- <sup>12</sup> A. Tsukernik, A. Palevski, V. J. Goldman, S. Luryi, E. Kapon, and A. Rudra, Phys. Rev. B 63, 153315(2001).
- <sup>13</sup> H. A. Ainspan and Keith A. Jenkins, IEEE JOURNAL OF SOLID-STATE CIRCUITS, 33, 2028(1998).
- <sup>14</sup> S. Iijima, Nature (London) 354, 36(1991).
- <sup>15</sup> A. V. Chaplik and R. H. Blick, New Journal of Physics 6, 33(2004).
- <sup>16</sup> J. Goldstone and R. L. Jaffe, Phys. Rev. B 45, 14100(1992).
- <sup>17</sup> A. I. Vedernikov and A. V. Chaplik, JETP 90,397(2000).
- <sup>18</sup> R. Dandoloff and T. T. Truong, Appl. Phys. A 325, 233(2004).
- <sup>19</sup> A. V. Chaplik, JETP Lett. 80, 130(2004).
- <sup>20</sup> S. Zhang, E. Zhang, S. Zhao, and M. Xia, Mod. Phys. Lett. A 18, 817(2004).
- <sup>21</sup> L. I. Magarill and A. V. Chaplik, JETP 88, 815(1999).
- <sup>22</sup> M. V. Entin and L. I. Magarill, Phys. Rev. B 64, 085330(2001).
- <sup>23</sup> R. C. T. da Costa, Phys. Rev. A 23, 1982(1981).
- <sup>24</sup> F. E. Meijer, A. F. Morpurgo, and T. M. Klapwijk, Phys. Rev. B 66, 033107(2002).
- <sup>25</sup> M. P. Trushin and A. L. Chudnovskiy, cond-mat/0505104(2005).
- <sup>26</sup> Y. V. Pershin and C. Piermarocchi, cond-mat/0507698(2005).
- <sup>27</sup> S. Griffith, Trans. Faraday Soc. 49, 345(1953).
- <sup>28</sup> J. B. Xia, Phys. Rev. B 45, 3593(1992).
- <sup>29</sup> D. Grundler, Phys. Rev. Lett. 84, 6074(2000).
- <sup>30</sup> J. Nitta, T. Akazaki, H. Takayanagi, and T. Enoki, Phys. Rev. Lett. 78, 1335(1997).

Fig. 1 (E. Zhang et al)

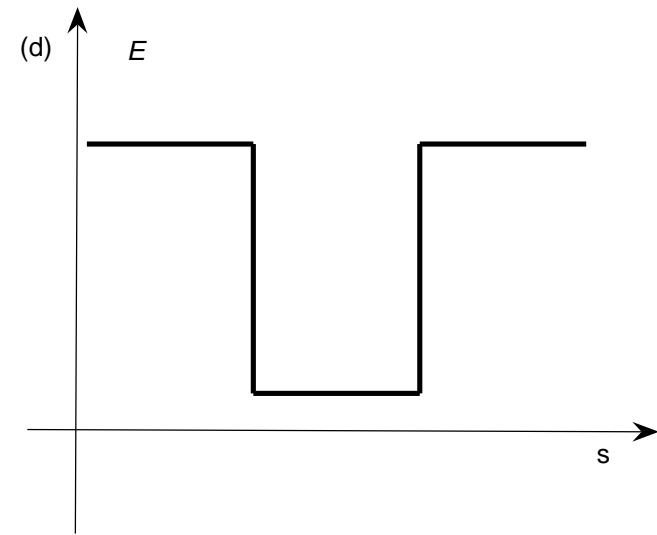
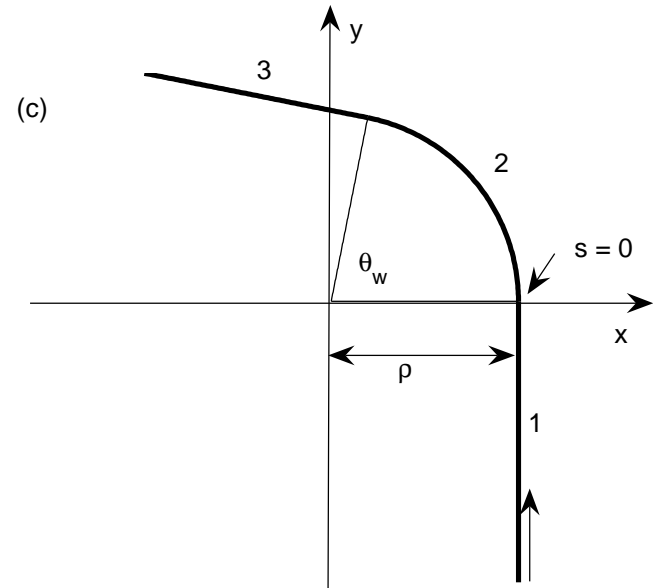
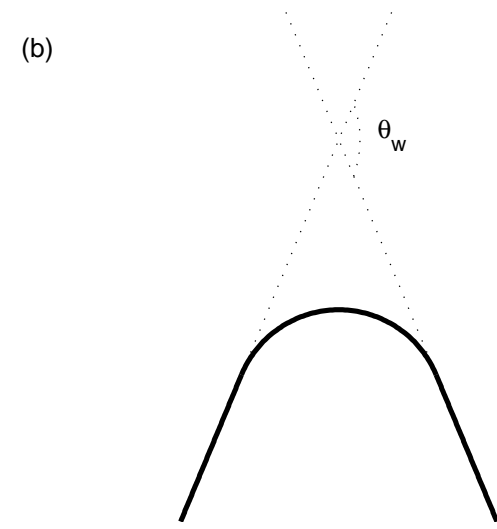
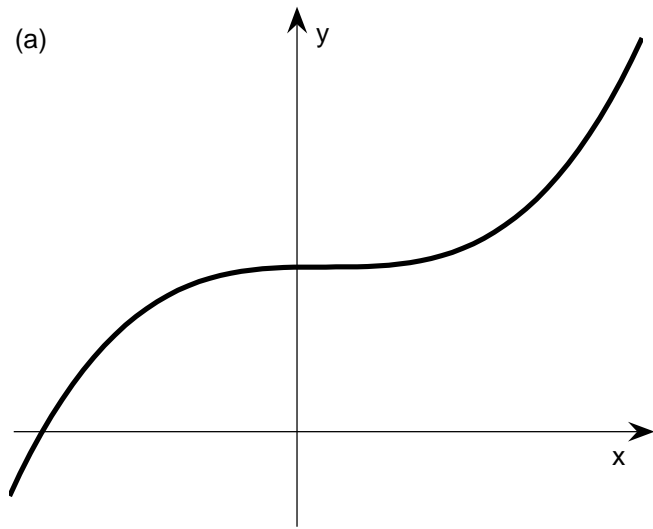




Fig. 2 (E. Zhang et al)

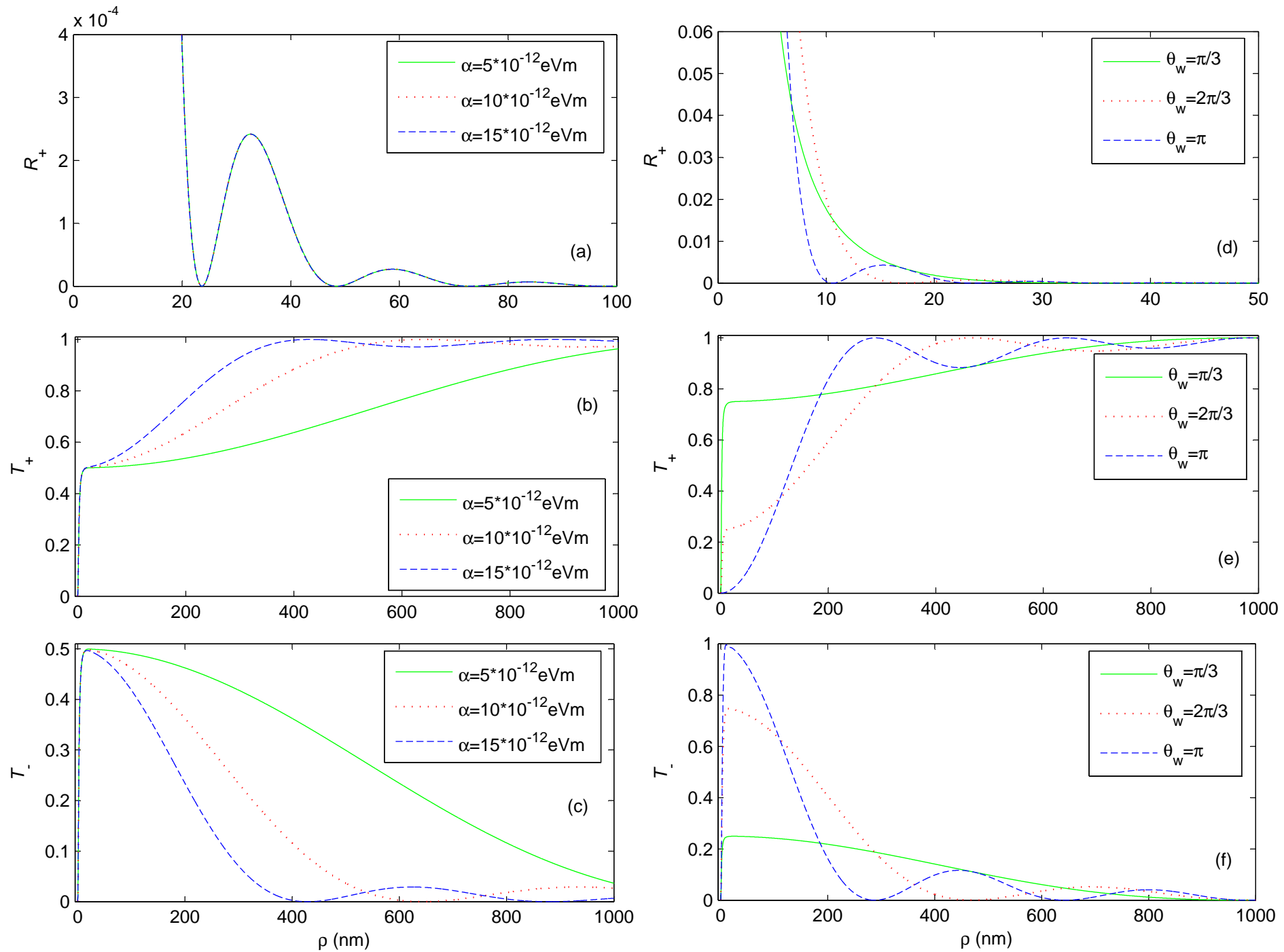


Fig. 3 (E. Zhang et al)

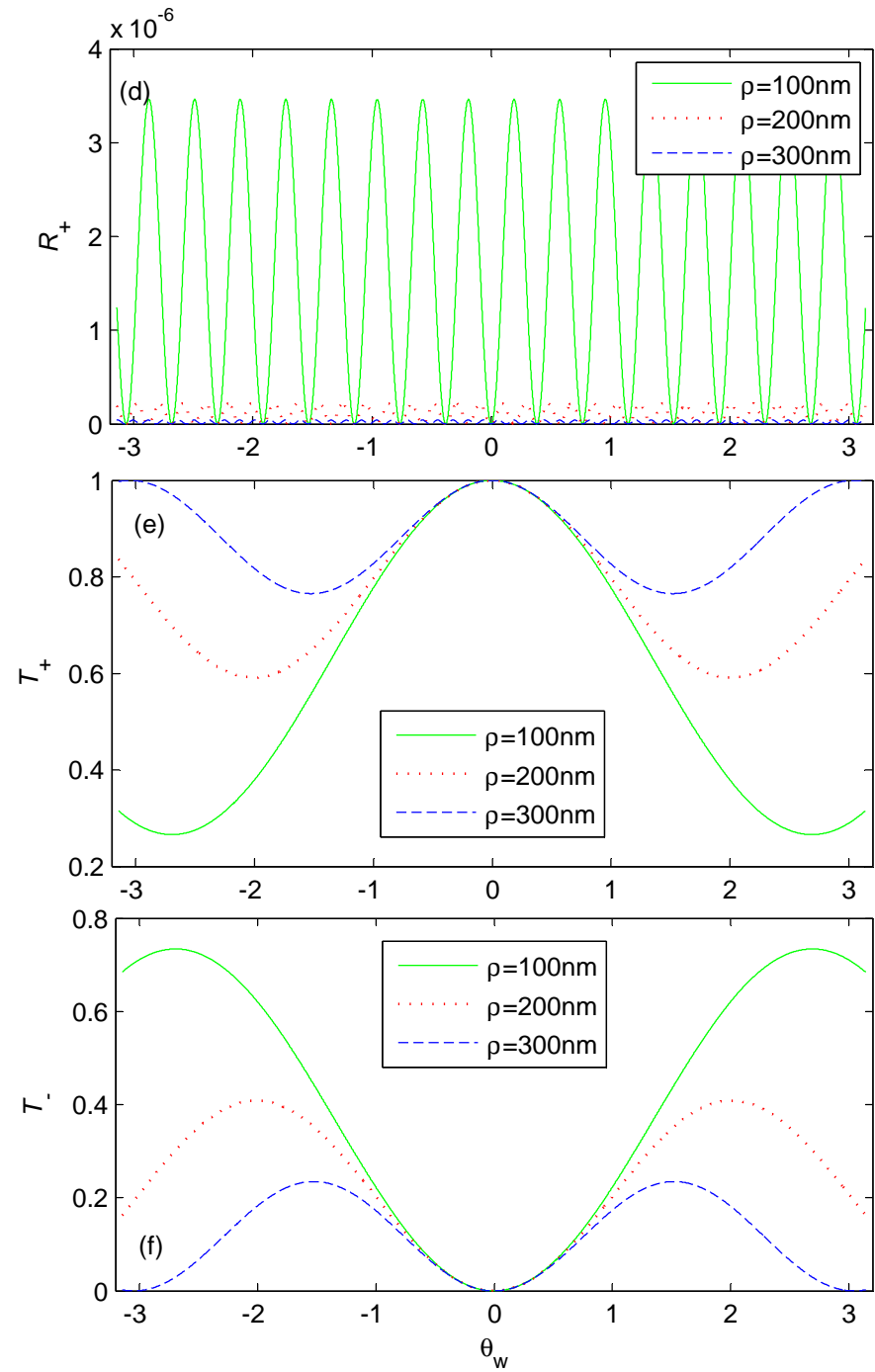
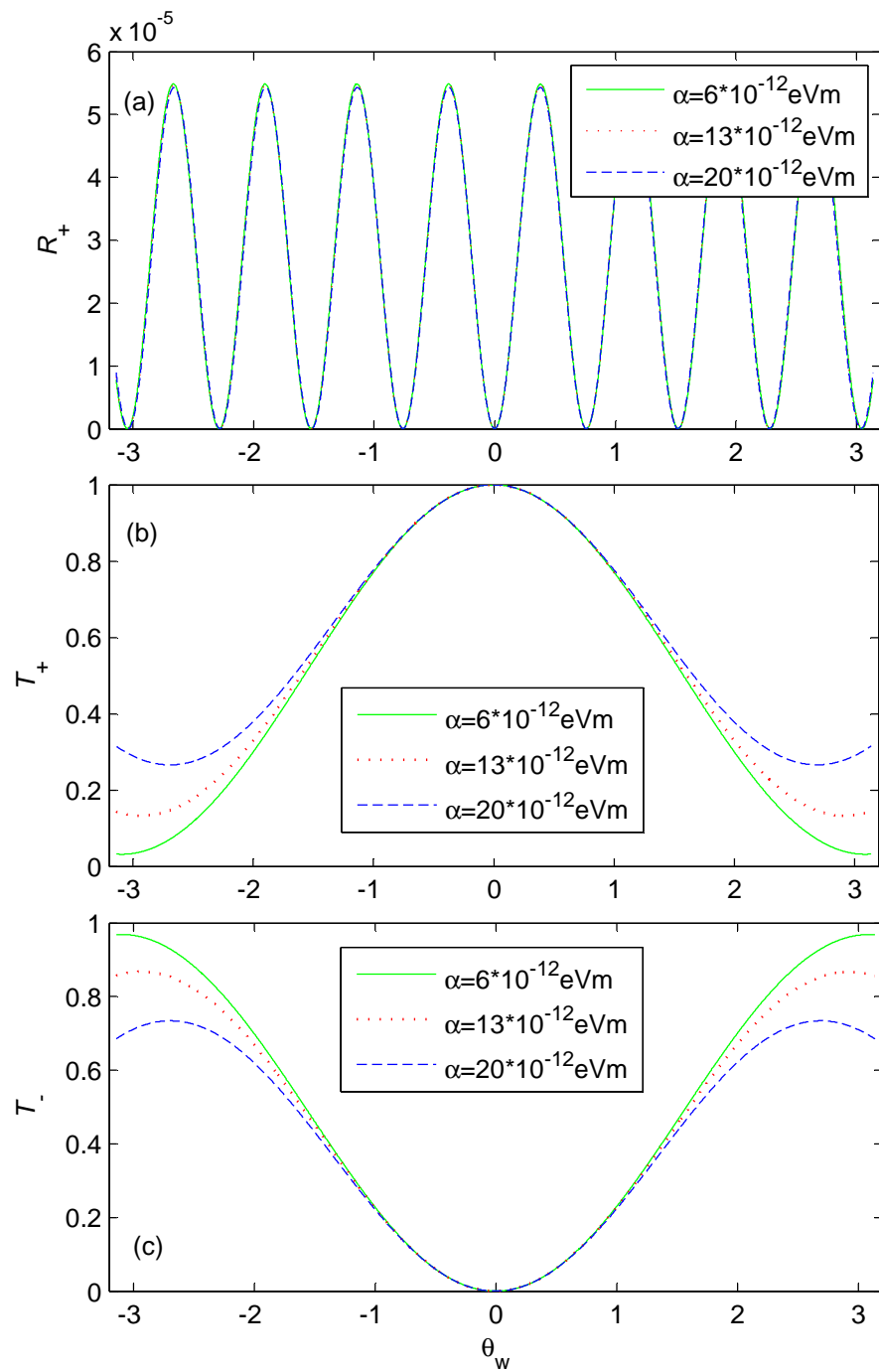


Fig. 4 (E. Zhang et al)

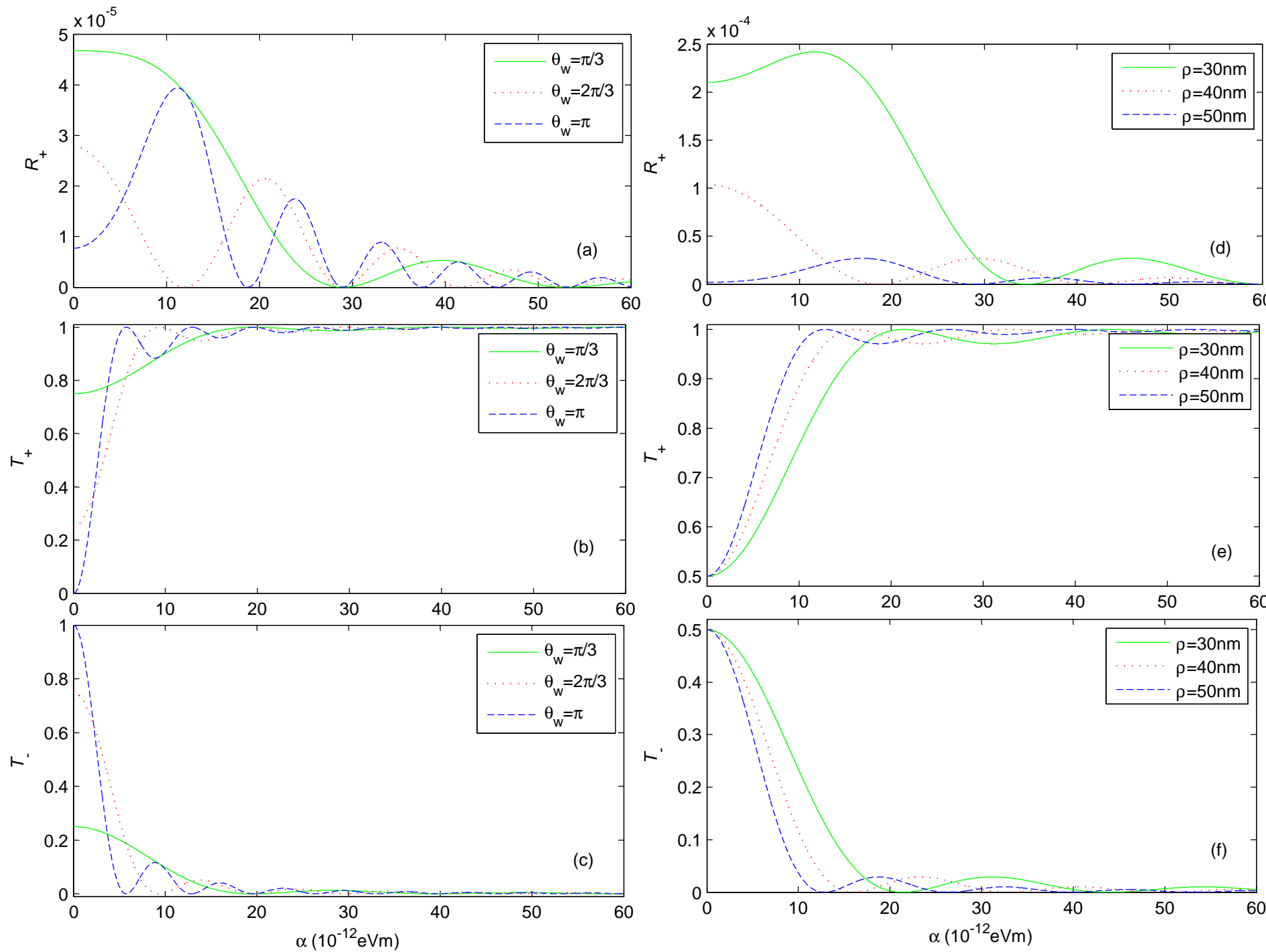


Fig. 5 (E. Zhang et al)

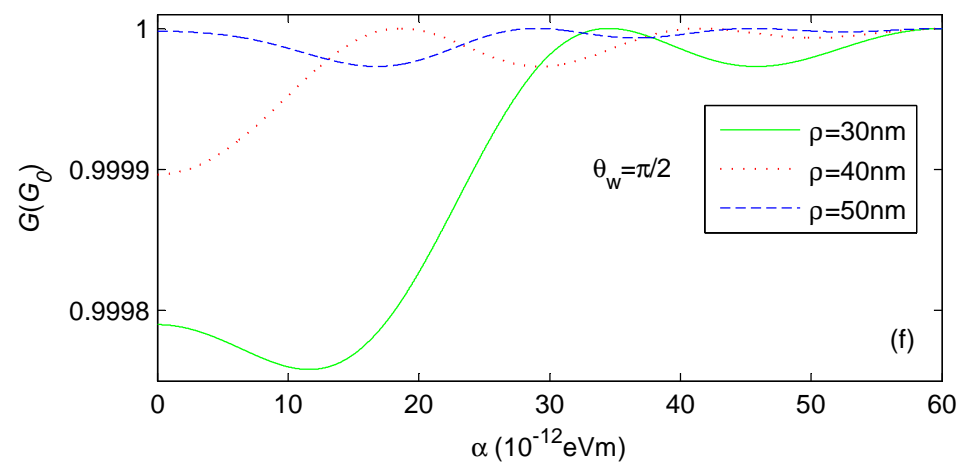
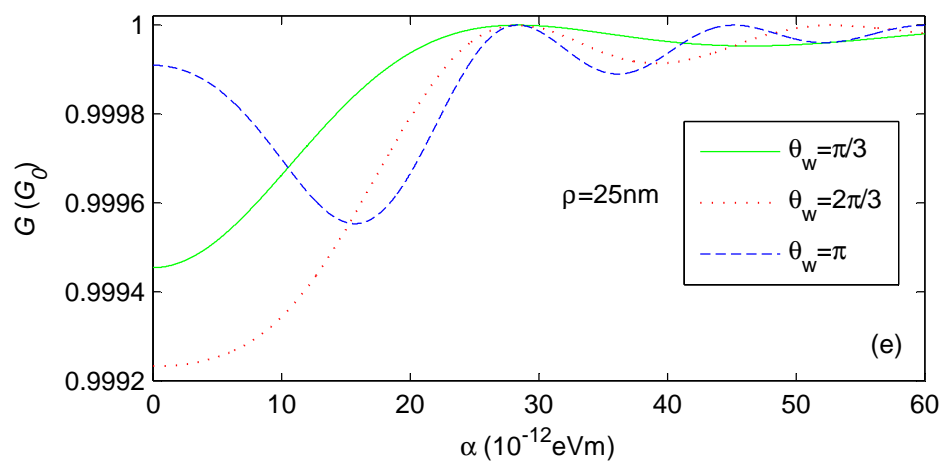
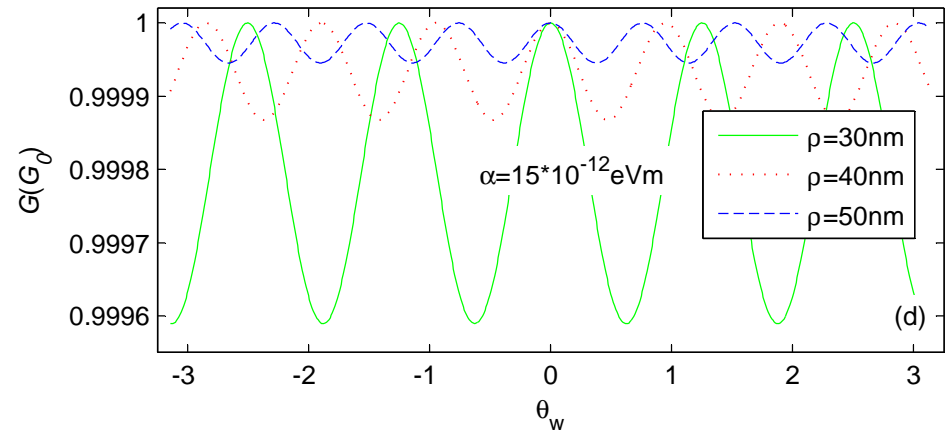
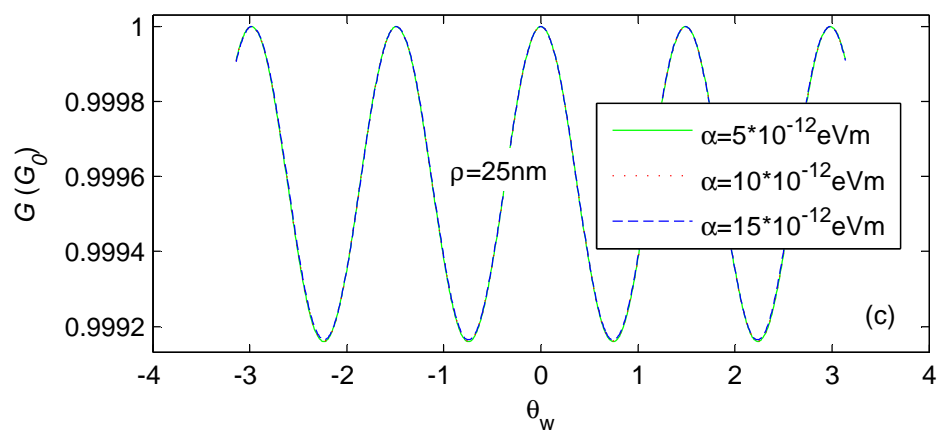
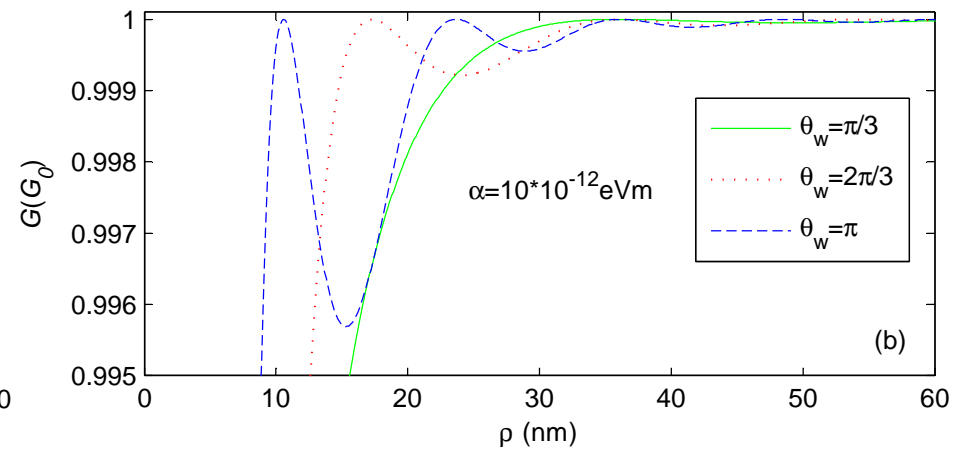
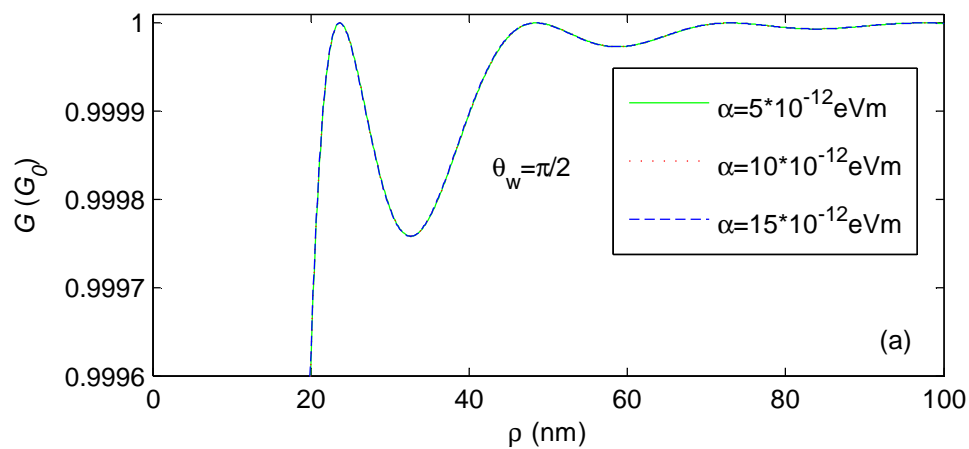


Fig. 6 (E. Zhang et al)

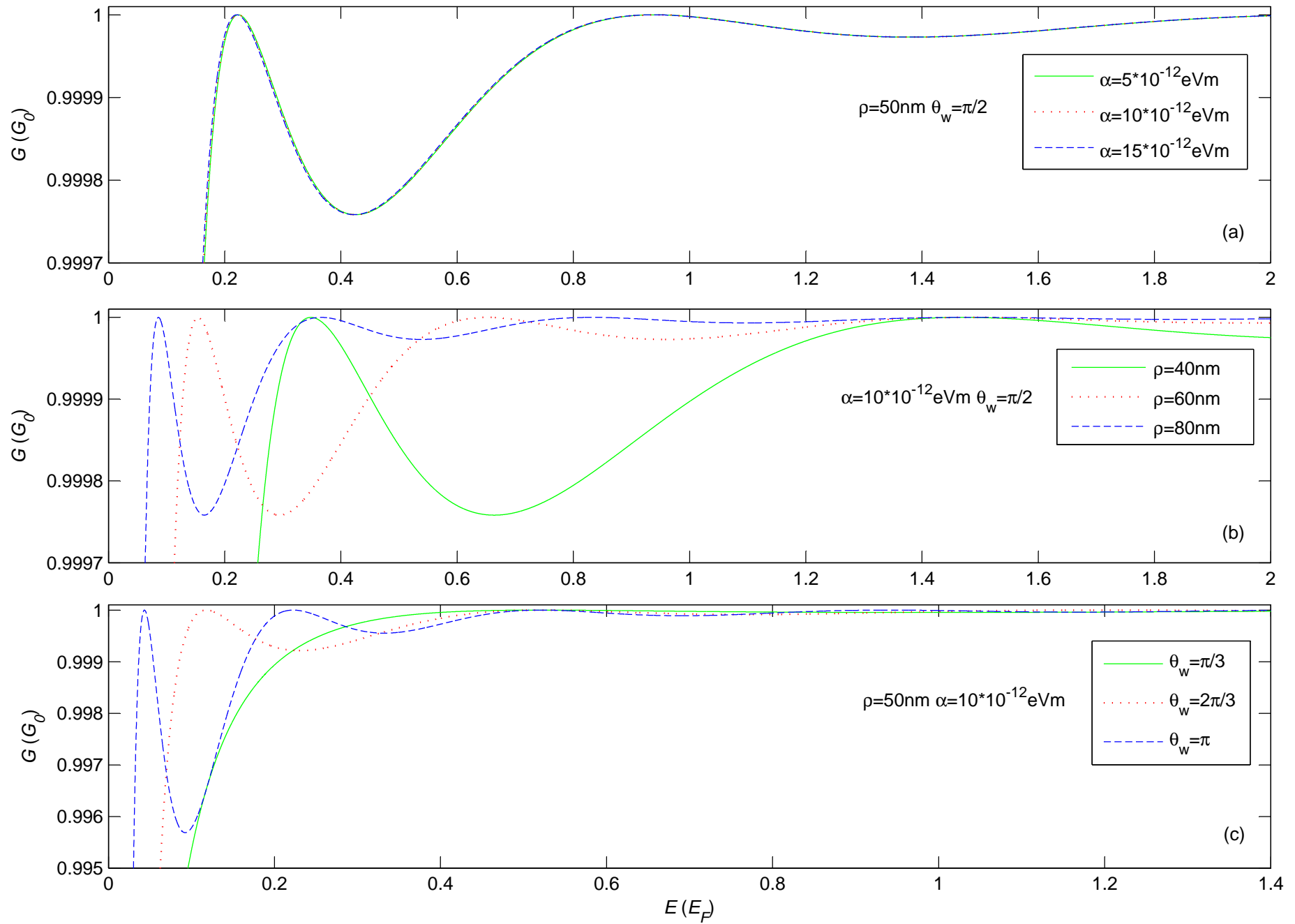


Fig. 7 (E. Zhang et al)

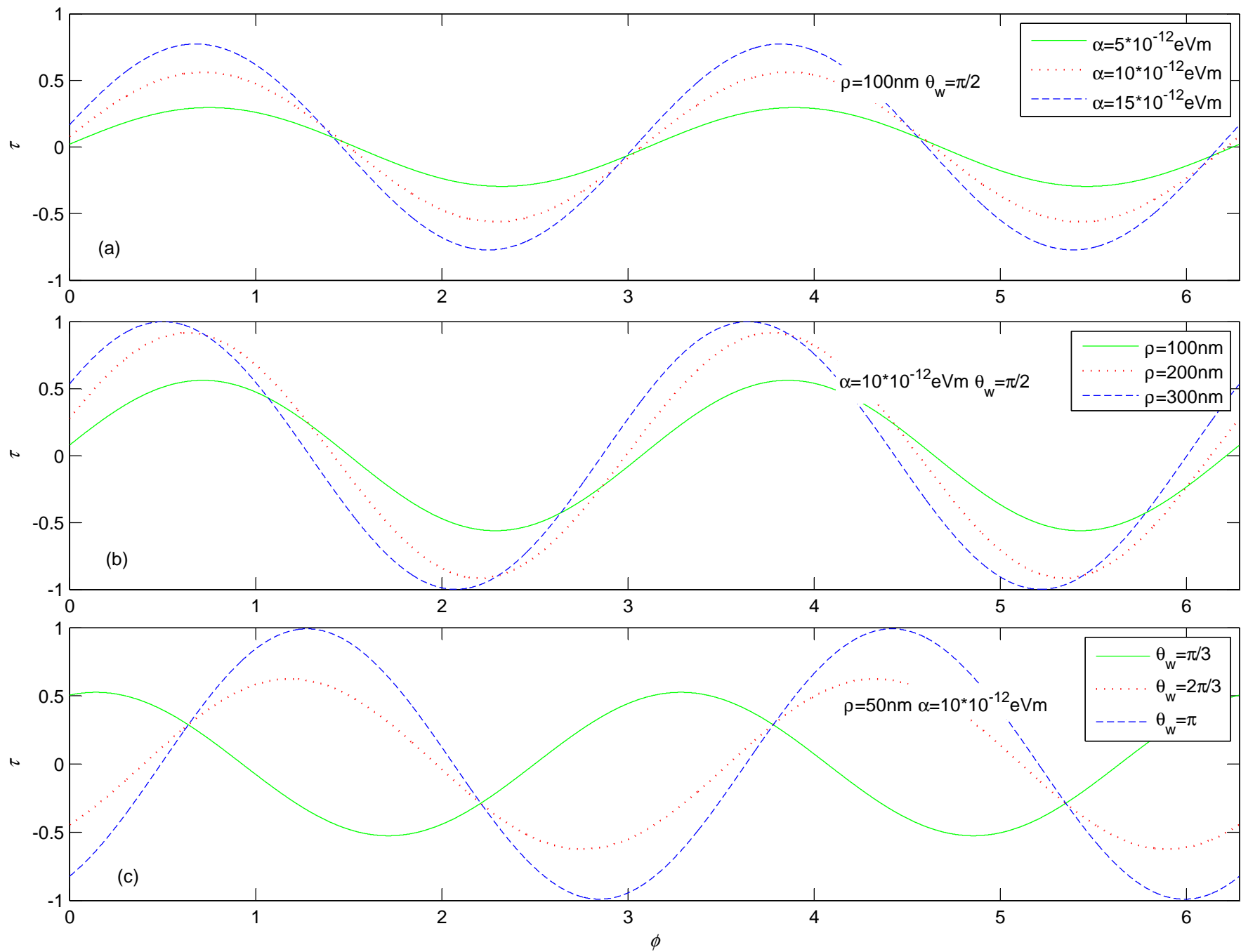


Fig. 8 (E. Zhang et al)

